Structure investigation with the (*p,t*) reaction on ^{132,134}Ba nuclei

S. Pascu,[1,2] Gh. Căta-Danil,[1,2] D. Bucurescu,[1,3] N. Mărginean,[1] C. Müller,[2] N. V. Zamfir,[1] G. Graw,[4] A. Gollwitzer,[4] D. Hofer,[4] and B. D. Valnion[4]

[1]*National Institute for Physics and Nuclear Engineering, RO-77125 Bucharest-Magurele, Romania*
[2]*Physics Department, Politehnica University of Bucharest, RO-060042 Bucharest, Romania*
[3]*Academy of Romanian Scientists, 54 Splaiul Independentei, RO-050094 Bucharest, Romania*
[4]*Fakultät für Physik der Universität München, D-85748 Garching, Germany*

(Received 20 October 2009; published 13 January 2010)

The low-lying excited states in ^{132,134}Ba isotopes have been studied with high-resolution (p,t) reactions. The experiments were performed at the Munich Q3D spectrograph with a 25-MeV proton beam and the 1.5-m-long focal plane detector. The high-resolution triton spectra allowed the observation of levels up to ∼4 MeV. The experimental results revealed 75 excited states in ^{134}Ba and 79 in ^{132}Ba, many of them observed for the first time. The measured angular distributions compared with distorted-wave Born approximation calculations allowed spin assignments for these levels in most cases. The systematics of the monopole and quadrupole two-neutron transfer strengths is compared with the prediction of the interacting boson approximation model. The results indicate a transitional structure in ^{132}Ba and ^{134}Ba and contribute additional evidence in favor of a description between the U(5) and O(6) symmetries of the model.

DOI: 10.1103/PhysRevC.81.014304 PACS number(s): 21.10.−k, 21.60.Ev, 25.40.Hs, 27.60.+j

I. INTRODUCTION

The nuclei ^{132}Ba and ^{134}Ba are placed in a typical transitional region of the nuclear chart along the U(5)-O(6) leg of the symmetry triangle [1] of the interacting boson approximation (IBA-1) model [2]. More recent studies [3] found fingerprints of an E(5) critical point symmetry in ^{134}Ba. Therefore, detailed knowledge of the low-lying states is needed to better understand the structure of these nuclei. It is well known that (p,t) reactions provide a rather detailed description for the low spin levels in even-even nuclei. For example, in a recent study on ^{128}Ba, the information on the low-lying levels was considerably improved by using a (p,t) reaction [4]. Therefore, in the present work the ^{136}Ba$(p,t)^{134}$Ba and ^{134}Ba$(p,t)^{132}$Ba reactions were selected to populate the low-lying states of the residual nuclei. A previous study [5] focused on the 0^+ states in ^{132}Ba and ^{134}Ba. The present work addresses mainly $L > 0$ transfers. The comparison between the experimental angular distributions and distorted-wave Born approximation (DWBA) calculations allowed spin assignments for most of these levels. From this comparison, two-neutron transition strengths were extracted for the 0^+ and 2^+ states, which were compared with the IBA-1 model predictions by employing a new set of model parameters. These parameters simultaneously describe the existing electromagnetic data and the present hadronic ones. This comparison indicates from both perspectives that the structure of the ^{132}Ba and ^{134}Ba nuclei is close to the prediction of the O(6) symmetry of the model [6]. This result confirm the previous structure assignment made on the basis of γ-ray spectroscopic data [1] and hadronic data [5]. Two other neighboring even-even nuclei, ^{128}Ba and ^{130}Ba, recently investigated via the (p,t) reactions (Refs. [4] and [7]) also show a structure resembling that of the O(6) symmetry. Both the experimental and theoretical data for these four nuclei support the idea, discussed in Ref. [1] and reiterated in Ref. [7], that Ba isotopes in the $N < 82$ region pass through a transitional structure located between vibrational [U(5)] nuclei and γ-soft nuclei [O(6)].

II. EXPERIMENTAL CONDITIONS

The experiments were performed with a 25-MeV proton beam delivered by the MP Tandem accelerator of the Maier-Leibnitz Laboratory of Ludwig Maximilians University and Technical University of Munich. The emerging tritons were momentum analyzed using the Q3D spectrograph [8] and detected in its focal plane by a 1.5-m-long multidetector system [9] composed of three proportional counters and a plastic scintillator to measure their residual energy. The focal-plane detector provides particle identification and background reduction, accepting only events within the correct angle of incidence. The energy resolution obtained was 5–10 keV, which was determined mainly by the target thickness. In the present work, only the relative values of the measured cross sections are given. The absolute values are not reliable because of an inconsistency that occurred in the normalization of the experimental spectra. However, the conclusions of the present article, based only on the relative values of the cross sections, are not affected.

A. Results in ^{132}Ba

The good energy resolution of the spectrograph allowed 79 states to be resolved up to an excitation energy of ∼4.2 MeV with two magnetic settings of the spectrograph, partially overlapping. The first (lower-energy) magnetic setting covered an excitation range from ground state to ∼2800 keV. The second (higher-energy) magnetic setting covered an excitation energy from ∼1900 to ∼4200 keV. The ^{134}Ba target with thickness of 100 μg/cm^2, implanted into 30 μg/cm^2 carbon foils, was prepared at the PARIS isotope separator at Orsay. Typical beam currents were ∼500 nA. The experimental cross sections were obtained by normalizing the area of the peaks

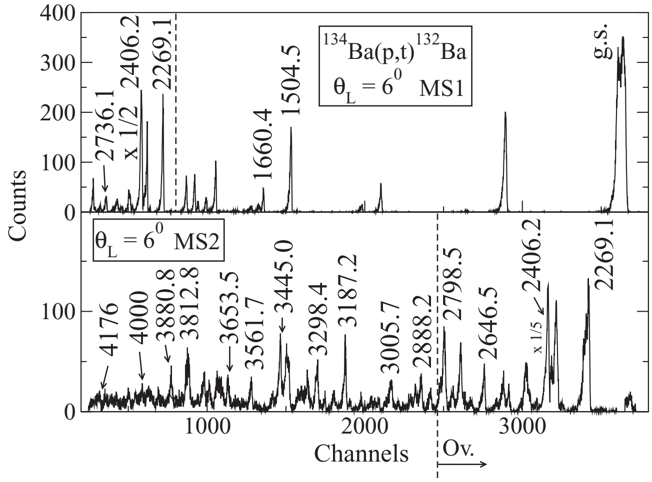

FIG. 1. Triton spectra from the ^{134}Ba$(p,t)^{132}$Ba reaction measured with the first magnetic setting (upper panel) and with the second magnetic setting (lower panel) of the Q3D spectrograph, measured at the laboratory angle of 6°. The incident energy of the protons was 25 MeV. The energies of the strong 0^+ excited levels are indicated in the figure. The vertical dashed line and the horizontal arrow placed below the figure and labeled "Ov." indicate the overlapped region of the two spectra.

from the spectra to the solid angle, the target thickness, and the beam charge obtained by integrating the beam current into the Faraday cup placed behind the target.

For the ^{134}Ba target, spectra were measured at ten angles between 6° and 50°. The spectra measured at 6° and 15° were recorded with both magnetic settings. Spectra measured at all other angles were collected with the second magnetic setting. Because the low-lying scheme of this nucleus is well known [10], the effort of the present work concentrated on extending the level scheme at higher energies. The spectrum recorded in the first magnetic setting was used only for its region that overlapped with the second magnetic setting for energy calibration purposes. The upper panel of Fig. 1 presents an example of the triton spectrum measured in the first magnetic setting at 6°, and the lower panel of Fig. 1 presents a spectrum recorded in the second magnetic setting at 6°.

For the spectra obtained using both magnetic settings, an internal energy calibration was performed. For ^{132}Ba, a third-order polynomial was used by taking the energies of the nuclear states obtained in previous γ-ray experiments [10] for the calibration peaks. This internal calibration relies on energy levels up to 3880.8 keV. For the remaining peaks, a linear extrapolation was performed up to 4176 keV because the angular distributions of the peaks above 3880.8 keV are reliable and give confidence that the observed states belong to ^{132}Ba. An uncertainty of 10 keV was assumed for the energies of these states. Table I summarizes the excitation energies for ^{132}Ba, as deduced from the present study.

B. Results in ^{134}Ba

For ^{134}Ba, 75 states were observed up to an excitation energy of ~3.9 MeV in two magnetic settings of the spectrograph covering excitation ranges similar to those for ^{132}Ba. The ^{136}Ba

TABLE I. Excitation energy, spin-parity, and relative $2n$ transfer intensity (see Sec. IV) for ^{132}Ba obtained in the present work, compared with the adopted values from Ref. [10]. The normalization for the $2n$ transfer strengths of the 0^+ and 2^+ states is chosen such that $\epsilon = 100\%$ for transition to the ground state and $\epsilon = 100\%$ for the first 2^+ state.

Ref. [10]		Present work		
E_{ex} (keV)	J^π	E_{ex} (keV)	J^π	ϵ (%)
0.0	0^+	0.0		100
464.508(12)	2^+	464.45(8)		100
1031.672(10)	2^+	1031.5(2)		21.4(21)
1127.615(18)	4^+	1128.0(4)		
1503.63(5)	0^+	1504.5(1)		1.3(3)
1660.30(4)	0^+	1660.4(2)		0.3(1)
1685.753(19)	2^+	1687.1(5)		5.7(5)
1729.343(20)	4^+	1730.4(3)		
1944.29(3)	(4^+)	1942.0(1)		
1998.179(22)	2^+	1998.7(3)		11.5(6)
2046.23(4)	2^+	2047.8(3)		6.6(3)
2068.553(21)	3^-	2069.1(2)		
2119.59(4)	5^-	2120.8(2)		
2271(8)	0^+	2269.1(1)		1.2(3)
2374.422(20)	3^-	2373.8(1)	2^+	26.8(12)
		2393.1(4)	2^+	37.6(12)
2406(8)	0^+	2406.2(1)	0^+	4.7(6)
2483.06(6)	7^-	2485.3(3)	(4^+)	
2492.35(8)	4^+	2491.6(6)	(4^+)	
		2553.1(3)	2^+	10.0(9)
		2573.6(3)		
		2599.9(6)	4^+	
		2646.5(2)	4^+	
2736(8)	0^+	2736.1(2)	0^+	0.4(2)
		2767.0(4)	4^+	
		2798.5(2)	2^+	35.0(14)
2855.84(5)	2^-	2852.5(4)	2^+	8.7(8)
2886(8)	0^+	2888.2(3)	(2^+)	12.8(7)
		2910.5(6)	(4^+)	
		2931.2(8)	2^+	4.4(5)
		2955.1(7)	2^+	1.2(4)
		2977.5(7)	(4^+)	
		2994.4(19)	(3^-)	
		3005.7(4)	0^+	0.2(1)
		3055.4(4)	2^+	2.7(7)
3068.79(12)	$1^+, 2^+, 3, 4^+$	3071.3(6)	2^+	2.3(6)
3082.94(20)		3086.3(6)	(4^+)	
		3123.6(4)	3^-	
		3167.7(4)	2^+	3.1(6)
		3187.2(2)	2^+	21.4(10)
3229.44(13)	(6^+)	3229.7(5)	2^+	5.3(6)
		3268.2(4)	4^+	
		3286.3(10)		
		3298.4(2)	2^+	14.7(9)
		3322.1(5)	2^+	3.0(7)
		3336.0(3)	2^+	10.0(8)
		3349.3(12)	4^+	
3363.55(21)	$1, 2^+$	3361.4(6)		
		3375.3(6)		
3412(8)	0^+	3411.4(3)	0^+	0.4(1)
		3421.3(5)	(0^+)	0.3(1)

TABLE I. (*Continued.*)

Ref. [10]		Present work		
E_{ex} (keV)	J^π	E_{ex} (keV)	J^π	ϵ (%)
3445(8)	0^+	3445.0(2)	0^+	0.5(2)
		3476.5(5)		
		3506.1(6)	2^+	0.5(1)
		3528.9(8)	4^+	
		3543.8(9)		
		3561.7(3)	3^-	
		3581.6(8)	2^+	0.9(2)
		3595.1(9)		
		3630.4(7)		
		3653.5(3)	2^+	6.8(6)
		3679.8(3)	0^+	0.10(5)
		3727.5(4)		
3751(8)	0^+	3751.8(4)	0^+	0.2(1)
3812(8)	0^+	3812.8(4)	0^+	0.3(1)
3834.78(12)	$1, 2^+$	3836.1(6)	2^+	4.3(6)
		3849.1(12)	3^-	
		3860.2(10)		
3882(8)	0^+	3880.8(4)	0^+	0.2(1)
		3932(10)		
		3962(10)		
		3978(10)	2^+	2.8(6)
		4000(10)	(0^+)	0.3(1)
4027.74(11)	$2^+, 3, 4^+$	4029(10)	(2^+)	5.5(7)
		4053(10)	2^+	2.4(5)
		4099(10)		
		4123(10)		
		4147(10)	(2^+)	4.5(6)
		4176(10)	(2^+)	5.7(6)

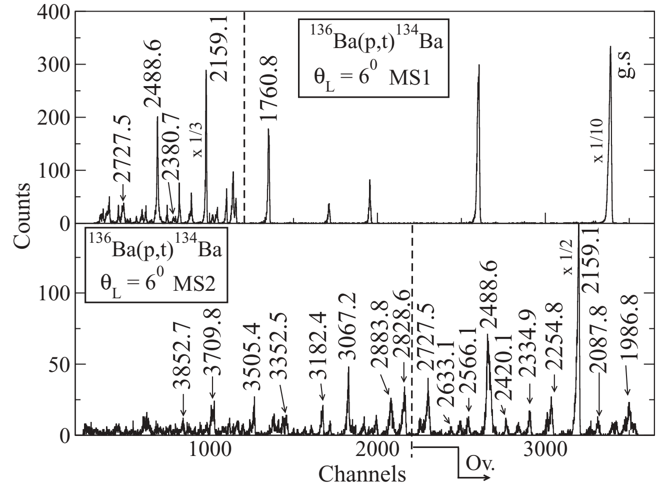

FIG. 2. Illustration of the energy spectra of ^{134}Ba measured with the first magnetic setting (upper panel) and the second magnetic setting of the magnetic Q3D spectrograph (lower panel). The numbers displayed in the figure are the energies obtained by an internal procedure for energy calibration that was employed for both nuclei (see text). The vertical dashed line and the horizontal arrow placed below the figure and labeled "Ov." indicate the overlapped region of the two spectra.

target with thickness 100 μg/cm^2, implanted into 30 μg/cm^2 carbon foil, was also prepared in the PARIS isotope separator at Orsay. Typical beam currents were ~300 nA.

For the ^{136}Ba target, the spectra were recorded only at 6°, 15°, and 30° for both magnetic settings of the spectrograph because the primary interest was to find new 0^+ states. The upper panel of Fig. 2 presents examples of the triton spectra measured with the first magnetic setting at 6° and the lower panel presents a spectrum recorded with the second magnetic setting at 6°.

An internal energy calibration was performed for the spectra obtained in both magnetic settings. A third-order polynomial was employed by using the energies of the nuclear states obtained in previous γ-ray experiments [11] for calibration. This internal calibration relies on energy levels up to 3852.7 keV. Table II summarizes the excitation energies for ^{134}Ba as deduced from the present study.

III. ANGULAR DISTRIBUTIONS AND THEIR DWBA ANALYSIS

The angular distributions of tritons measured in the present work (relative values) are presented in Fig. 3 for ^{132}Ba. To extract the value of the transferred angular momentum, we compared the experimental angular distributions with calculations made with the DWBA [12]. The numerical calculations were performed with the DWUCK-4 computer code [13] assuming a direct, single-step process for the (p,t) reaction. The optical model parameters employed for protons and tritons for ^{132}Ba were taken from Ref. [14]. The potential used for ^{134}Ba is similar to that used in Ref. [14]. The form of the potential includes a volume Woods-Saxon term, a surface derivative potential, and a spin-orbit term. The well depths are given in MeV as follows: for protons, the real volume potential is 50, the imaginary term is 2.1, the imaginary derivative potential is 10, and the real spin-orbit term is 3; for tritons, the real volume potential is 176 and the imaginary term is 18. For the transfer of the two neutrons, experiments were performed similarly to Ref. [7] by considering a cluster form factor in the neutron configuration $(1h_{11/2})^2$ for L = even and $(1h_{11/2}, 1g_{7/2})$ for L = odd. Alternative form factors such as $(2d_{3/2})^2$, $(1g_{7/2})^2$, or $(3s_{1/2})^2$ for L = even and $(1h_{11/2}, 2d_{5/2})$ for L = odd give similar shapes and the same pattern of the relative normalization factors.

As can be seen in Fig. 3, the DWBA calculations give a good description for most of the angular distributions, leading to unambiguous L assignments for ^{132}Ba. For some of the levels where the experimental cross sections are small, the angular distributions appear structureless. This is the case for twelve levels which have the energies 2573.6, 3286.3, 3361.4, 3375.3, 3476.5, 3543.8, 3630.4, 3727.5, 3860.2, 3932.3, 4099, and 4123 keV, and may indicate that they are populated not by a direct process but by multistep processes.

For the levels from ^{134}Ba only three angles were measured. Examples of angular distributions are given in Fig. 4 for each value of the transferred angular momentum. For the measured levels, the (sometimes tentative) spin assignment was based on the values of the ratio $R_\sigma = \sigma(6°)/\sigma(15°)$ of the differential

TABLE II. Excitation energy, spin-parity, and relative $2n$ transfer intensity (see Sec. IV) for ^{134}Ba obtained in the present work, compared with the adopted values from Ref. [11]. $R_\sigma = \sigma(6^\circ)/\sigma(15^\circ)$ is the ratio of the differential cross sections at the laboratory angles of 6° and 15°. The normalization for the $2n$ transfer strengths is chosen in the same way as for ^{132}Ba (Table I).

Ref. [11]		Present work			
E_{ex} (keV)	J^π	E_{ex} (keV)	R_σ	J^π	ϵ (%)
0.0	0^+	0.0	7.0	0^+	100
604.7223(19)	2^+	604.8(1)	0.3	2^+	100
1167.968(3)	2^+	1167.4(4)	0.6	$2^+, 3^-$	8.2(3)
1400.590(3)	4^+	1399.7(3)	1.3	4^+	
1760.555(22)	0^+	1760.8(3)	6.1	0^+	2.6(1)
1969.921(4)	4^+	1970.2(3)	1.0	4^+	
1986.35(21)	5^-	1986.8(2)	0.7	5^-	
2029.242(18)	2^+	2029.2(1)	0.2	2^+	11.7(4)
2088.288(17)	2^+	2087.8(1)	0.2	2^+	9.5(4)
2118.195(9)	(4^+)	2117.2(4)	1.2	4^+	
2159.683(21)	$(0)^+$	2159.1(2)	9.8	0^+	8.8(3)
2254.95(14)	3^-	2254.8(2)	0.6	3^-	
2271.57(24)	7^-	2272.1(3)	0.8	7^-	
2334.76(6)	$1,2^+$	2334.9(1)	0.4	2^+	12.2(4)
		2373.1(6)	1.6	4^+	
2379.112(18)	0^+	2380.7(9)	1.8	(0^+)	0.10(1)
		2420.1(3)	1.2	4^+	
2464.28(6)	(2^+)	2464.2(2)	0.4	2^+	2.7(2)
2479(10)	4^+	2480.8(2)	0.8	$3^-, 4^+$	
2488.434(21)	0^+	2488.6(1)	9.8	0^+	2.2(1)
		2535.6(8)	1.4	4^+	
2564.712(19)	$1^+, 2^+$	2566.1(2)	0.2	2^+	7.6(3)
		2587.0(10)	1.4	4^+	
2599.88(4)	2^+	2600.2(3)	0.4	2^+	3.2(2)
		2633.1(4)	1.1	4^+	
2677.76(8)	3,4	2679.1(6)	0.7	3^-	
		2702.5(7)	1.7	(4^+)	
2729.23(4)	$1,2^+$	2727.5(2)	3.2	0^+	1.0(1)
2747.965(24)	2^+	2747.9(2)	0.3	2^+	1.8(2)
2760.74(12)	$1,2^+$	2761.4(3)	0.5	(2^+)	3.5(2)
2828.50(4)	$1^+, 2^+$	2828.6(1)	0.4	2^+	15.6(5)
2851.26(6)	2^+	2849.6(6)	0.5	(2^+)	2.2(2)
		2873.4(5)	0.8	3^-	
2874(8)	0^+	2883.8(2)	7.9	0^+	0.8(1)
		2912.7(7)	0.6	3^-	
2943.90(14)	$2^+, 3^-, 4^+$	2944.7(3)	1.1	4^+	
		2961.1(12)	2.2	(0^+)	0.10(1)
		2975.5(7)	0.7	3^-	
2996(8)	0^+	3000.6(2)	4.4	0^+	0.3(1)
		3041.0(4)	0.3	2^+	1.6(2)
		3054.1(5)	0.2	2^+	2.7(2)
3068.85(13)	$1, 2^+$	3067.2(2)	1.1	4^+	
		3149.5(5)	1.2	4^+	
3181(8)	(0^+)	3182.4(2)	0.8	(3^-)	
		3231.5(6)	0.9	$(3^-, 4^+)$	
3262.0(3)	$2^+, 3^-, 4^+$	3264.0(6)	0.7	3^-	
		3292.9(7)	0.3	2^+	0.8(1)
3311.3(8)		3312.9(10)	0.9	$(3^-, 4^+)$	
		3352.5(3)	0.8	3^-	
3368.97(6)	1,2	3366.0(2)	0.3	2^+	4.5(3)
		3380.3(10)	1.7	(4^+)	

TABLE II. (*Continued.*)

Ref. [11]		Present work			
E_{ex} (keV)	J^π	E_{ex} (keV)	R_σ	J^π	ϵ (%)
		3395.1(10)	2.6	0^+	0.10(1)
3408.72(17)	1,2	3407.9(8)	0.2	2^+	2.6(2)
		3414.0(6)	0.6	3^-	
		3434.1(7)	0.7	3^-	
3501(8)	$(0)^+$	3505.4(5)	3.4	0^+	0.5(1)
		3519.2(3)	0.3	2^+	2.3(2)
		3555.0(7)	0.8	(3^-)	
		3577.7(5)	0.6	(3^-)	
		3602.3(11)	2.1	(0^+)	0.10(1)
3618(8)	$(0)^+$	3623.9(4)	2.0	(0^+)	0.4(1)
		3639.5(6)	0.8	(3^-)	
3652.1(5)	$1, 2^+$	3654.9(5)	1.0	4^+	
		3670.7(9)	0.5	(2^+)	0.5(1)
		3685.1(4)	0.2	2^+	1.2(1)
3705(5)	1	3709.8(4)	0.3	2^+	4.6(2)
		3722.4(10)	0.5	(2^+)	0.7(1)
		3737.8(8)	0.2	2^+	1.5(1)
3754(10)		3750.4(10)	2.0	(0^+)	0.2(1)
		3768.5(4)	1.2	4^+	
		3791.2(6)	1.0	(4^+)	
		3805.5(6)	0.6	3^-	
		3820.6(6)	1.2	4^+	
		3835.1(6)	0.7	3^-	
3853.8(4)	2^+	3852.7(2)	0.3	2^+	2.8(2)

cross section at the laboratory angles of 6° and 15°, which is a good spin signature, especially for 0^+ states. The criteria set for the ratio R_σ are taken from the DWBA calculations. The value is larger than 3.0 for $L = 0$ transitions, whereas for higher L transfer the ratios are significantly lower: $R_\sigma \simeq 0.3$ for $L = 2$, $R_\sigma \simeq 0.7$ for $L = 3$, and $R_\sigma \simeq 1.2$ for $L = 4$. J^π values reported in Table II are based on these R_σ values.

IV. DISCUSSION

Tables I and II summarize the experimental information obtained from the present study for ^{132}Ba and ^{134}Ba, respectively, in comparison with previous knowledge. The relative $2n$ transfer strengths, ϵ, of the $L = 0$ and $L = 2$ transitions are given for the 0^+ and 2^+ states. These strengths are defined as follows. For ^{132}Ba for which a full angular distribution was measured, (ten angles),

$$\left(\frac{d\sigma}{d\Omega}\right)_{\rm expt} = \epsilon \cdot \left(\frac{d\sigma}{d\Omega}\right)_{\rm DWBA}, \quad (1)$$

where $(d\sigma/d\Omega)_{\rm expt}$ is the experimental angular distribution and $(d\sigma/d\Omega)_{\rm DWBA}$ is the corresponding DWBA angular distribution. For ^{134}Ba for which the cross section was measured at only three angles, the $2n$ transfer strength for $L = 0$ is given by

$$\sigma_{\rm expt}(6^\circ) = \epsilon \cdot \sigma_{\rm DWBA}(6^\circ), \quad (2)$$

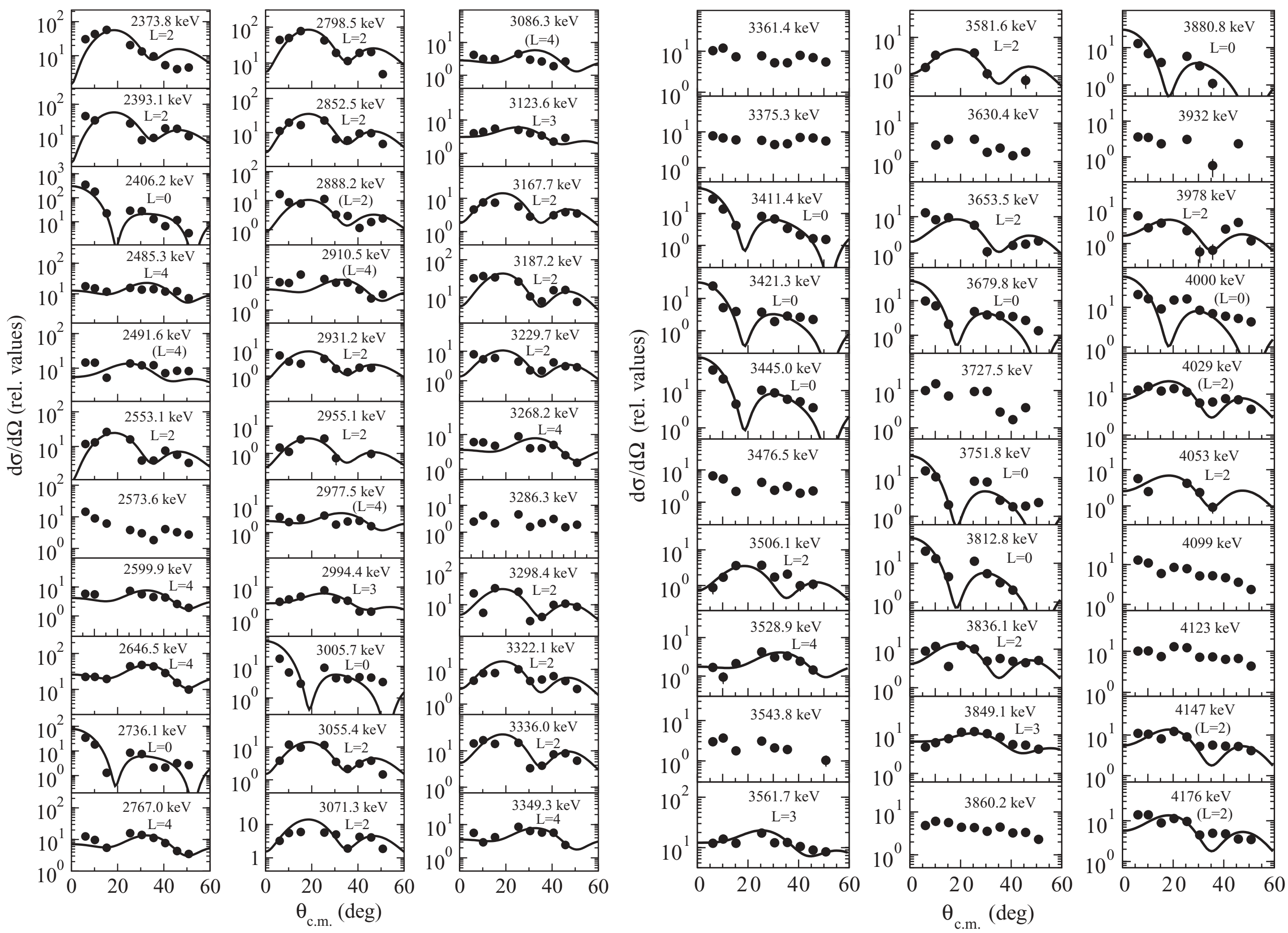

FIG. 3. Experimental angular distributions (points) and DWBA calculations (curves) for the transferred angular momenta $L = 0$, 2, 3, and 4 in the ^{134}Ba(p,t) ^{132}Ba reaction at 25 MeV. The experimental cross sections are given in relative units (see text for details). The error bars are smaller than the size of the dot for most of the angular distributions.

where $\sigma_{\text{expt}}(6^{\circ})$ is the experimental cross section at 6° and $\sigma_{\text{DWBA}}(6^{\circ})$ is the corresponding DWBA cross section, and for $L = 2$ is given by

$$\sigma_{\text{expt}}(15^{\circ}) = \epsilon \cdot \sigma_{\text{DWBA}}(15^{\circ}), \qquad (3)$$

where $\sigma_{\text{expt}}(15^{\circ})$ is the experimental cross section at 15° and $\sigma_{\text{DWBA}}(15^{\circ})$ is the corresponding DWBA cross section.

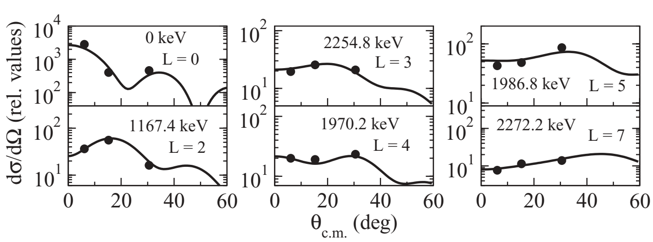

FIG. 4. Examples of experimental angular distributions (symbols) and DWBA calculations (curves) for the transferred angular momenta $L = 0$, 2, 3, 4, 5, and 7 in the ^{136}Ba(p,t) ^{134}Ba reaction at 25 MeV (see text for discussion).

The normalization is chosen separately for $L = 0$ and $L = 2$ transfers in both nuclei such that $\epsilon = 100\%$ for the ground state and the first excited 2^+ state, respectively.

The (p,t) reactions are a powerful tool for revealing the 0^+ states. In Ref. [4] it was shown that the number of known 0^+ states in ^{128}Ba was greatly improved as a result of the (p,t) study. Also, a systematic search of the Ba isotopes revealed that the number of known 0^+ states is many times higher in the nuclei where a (p,t) experiment was performed compared to the ones where no (p,t) study can be carried out. Thus, a similar situation is also expected for the experiments reported in the present work.

The two isotopes involved in this study show similar features. Up to 2 MeV, only one excited 0^+ state exists in ^{134}Ba and two excited 0^+ states in ^{132}Ba, with small intensities (a few percent of that of the ground state). A group of levels also exists close to the pairing gap. As discussed in Ref. [5], in the O(6) limit of the IBA-1, a vanishing (p,t) transfer is predicted to the first excited 0^+ state and a strong transfer (∼11% from that to the ground state) to the second excited 0^+. In the SU(3) limit of the model there is a strong transfer (∼35%) to the first excited 0^+ state and a vanishing excitation to the second excited 0^+ state. In the U(5) limit, the whole transfer strength is at the ground state, because the excited 0^+ states having zero intensity difference from that of the ground state. In this case, the experimental data obtained in the present work qualitatively place the ^{132}Ba and ^{134}Ba structure between these two limiting cases, but closer to O(6).

To obtain a numerical estimation of the relative (p,t) transfer strengths, the wave functions of the low-lying states in ^{132}Ba, ^{134}Ba, and ^{136}Ba were calculated in the IBA-1 model [2]. The IBA-1 Hamiltonian was diagonalized with the computer code PHINT and the electromagnetic matrix elements were calculated with the FBEM package [15]. The calculations were performed with a new set of parameters determined to reproduce all available experimental spectroscopic data in these nuclei. The available data preceding the present work [10,11] were obtained from γ-ray and hadronic probe spectroscopy in ^{132}Ba and ^{134}Ba. The electromagnetic data refer to excitation energies, branching ratios, transition probabilities, and mixing ratios of the γ transitions. Using definitions of bosonic operators from Ref. [2], the IBA-1 Hamiltonian employed in the present calculation is

$$\hat{H}_{sd} = \epsilon\hat{n}_d + \kappa(\hat{Q}\times\hat{Q})^{(0)} - 5\sqrt{7}\mathrm{OCT}\cdot[(\hat{d}^\dagger\tilde{d})^{(3)}\times(\hat{d}^\dagger\tilde{d})^{(3)}]^{(0)}. \quad (4)$$

where $\hat{Q}$ is the quadrupole operator given by

$$\hat{Q} = [(\hat{s}^\dagger\tilde{d} + \hat{d}^\dagger\hat{s})^{(2)} + \chi(\hat{d}^\dagger\tilde{d})^{(2)}] \quad (5)$$

and ϵ, κ, χ, and OCT are model parameters [2].

The electromagnetic transition operators are

$$\hat{T}(E2) = e_2\hat{Q}, \quad (6)$$

$$\hat{T}(M1) = \alpha_1[\hat{Q}\times\hat{L}]^{(1)} + \beta_1\hat{L}, \quad (7)$$

where e_2 represents the boson effective charge and α_1 and β_1 are other parameters [2].

The IBA-1 study reported in Ref. [5] used the O(6) limit of the model for ^{132}Ba to produce two excited states up to 2 MeV at excitation energies of roughly 1.2 and 1.7 MeV and a rather good agreement was concluded. The IBA-2 numerical study of Ref. [16] also predicts two 0^+ states below 2 MeV, at 1.521 and 1.925 MeV. This prediction is in reasonable agreement with the geometrical model study of ^{132}Ba in the general collective model, where two excited 0^+ states are expected at 1.569 and 2.485 MeV [17].

In the present work, the search for the model parameters started with the global values given in Ref. [18], where the extended consistent Q formalism (ECQF) was used. In a previous study of ^{128}Ba [4], to describe both electromagnetic and (p,t) data simultaneously with the ECQF Hamiltonian, it was found that it is essential to also consider the octupole term, whose strength is defined by the parameter OCT in Eq. (4). The properties of the 0_3^+ state are especially sensitive to this term. The effect of considering a nonvanishing value for the OCT parameter on the observables related to the 0_3^+ states is shown in Table III. The numerical values for the new parameters obtained in the present work are given in Table IV for ^{132}Ba, ^{134}Ba, and ^{136}Ba. The quality of the present calculation in describing the experimental data can be observed from Fig. 5 for electromagnetic data and from Figs. 6–9 for the hadronic data. The properties of the ground-state band [energies and $B(E2)$] and those of the quasi-γ band are well described. Also the calculated decay patterns of the excited 0^+ states are in reasonable agreement with the measured values, except for the second 0^+ state in ^{132}Ba.

With the wave functions obtained by diagonalizing the $\hat{H}_{sd}$ Hamiltonian [Eq. (4)] with the parameters of Table IV, the $2n$ transfer intensities between the ground states of ^{136}Ba and ^{134}Ba and the first four 0^+ states in ^{134}Ba and ^{132}Ba

TABLE III. The comparison between the experimental values of the sensitive observables of even-even Ba nuclei from ^{128}Ba to ^{136}Ba for the 0_3^+ states and the corresponding IBA-1 values with two sets of parameters. The parameters for calculation of set 1 are given in Table IV for ^{132}Ba, ^{134}Ba, and ^{136}Ba and are taken from Ref. [4] for ^{128}Ba and ^{130}Ba. The calculated data for ^{136}Ba are based on electromagnetic data from Ref. [19]. Set 2 takes the same values of parameters as those used in set 1 except for the OCT parameter, which was set to zero. $\epsilon_{0_3^+}$ are the $2n$ transfer intensities.

Nucleus	Obs.	Expt.	Set 1	Set 2
^{128}Ba	$E/E^{\mathrm{expt}}_{0_3^+}$	1	1.01	1.2
	$B(E2;0_3^+\to 2_1^+)$(W.u.)	1	10	0.4
	$B(E2;0_3^+\to 2_2^+)$(W.u.)	<1	18	78
	$B(E2;0_3^+\to 2_3^+)$(W.u.)	<33	1	5
	$\epsilon_{0_3^+}$	3.3(2)	5.1	0.8
^{130}Ba	$E/E^{\mathrm{expt}}_{0_3^+}$	1	0.8	1
	$\epsilon_{0_3^+}$	0.1	1.6	0.1
^{132}Ba	$E/E^{\mathrm{expt}}_{0_3^+}$	1	1.1	1.3
	$\frac{B(E2;0_3^+\to 2_2^+)}{B(E2;0_3^+\to 2_1^+)}$	8.5(9)	8.7	2770
	$\epsilon_{0_3^+}$	0.3(1)	2.3	0.2
^{134}Ba	$E/E^{\mathrm{expt}}_{0_3^+}$	1	0.95	1.4
	$B(E2;0_3^+\to 2_1^+)$(W.u.)	14^{+3}_{-14}	18	0.01
	$B(E2;0_3^+\to 2_2^+)$(W.u.)	2.5^{+8}_{-9}	5	47
	$\epsilon_{0_3^+}$	8.8(3)	1.6	0.01
^{136}Ba	$E/E^{\mathrm{expt}}_{0_3^+}$	1	1.1	1.6
	$\frac{B(E2;0_3^+\to 2_2^+)}{B(E2;0_3^+\to 2_1^+)}$	0	0.6	∞

TABLE IV. The IBA-1 parameters (for $\hat{H}_{\mathrm{sd}}$, $\hat{T}(E2)$, and $\hat{T}(M1)$) for ^{132}Ba, ^{134}Ba, and ^{136}Ba (see text for details).

Parameter	Nucleus		
	^{132}Ba	^{134}Ba	^{136}Ba
ϵ	0.7	0.95	1.05
κ	−0.04	−0.04	−0.04
χ	−0.303	−0.303	−0.303
OCT	−0.012	−0.028	−0.028
e_2	0.134	0.143	0.150
α_1	0.004	0.004	0.004
β_1	0.05	0.05	0.05

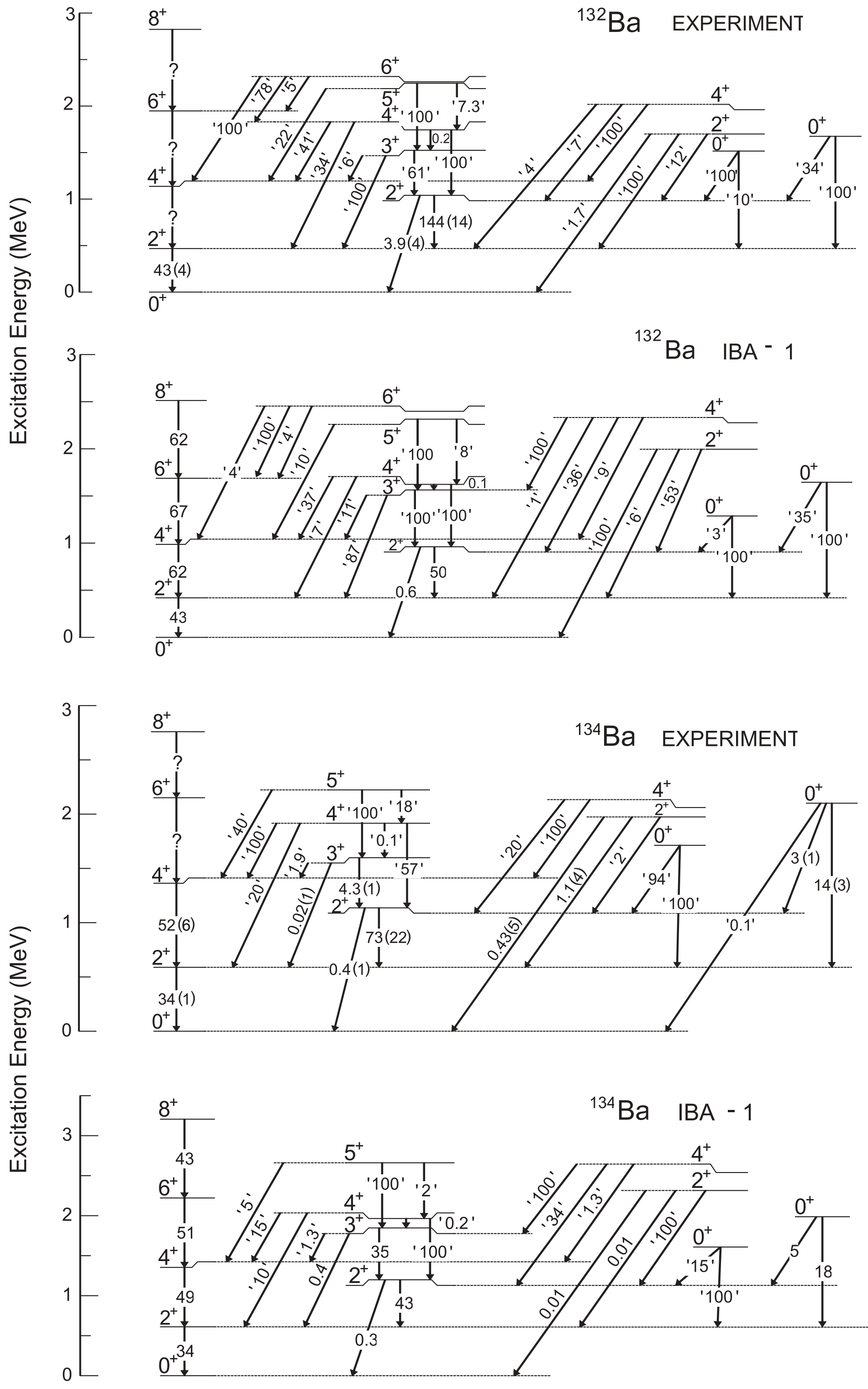

FIG. 5. Experimental excitation energies and transition probabilities or relative intensities of the γ-ray transitions for the low-lying levels of ^{132}Ba and ^{134}Ba compared with the present IBA-1 model calculation. The known $B(E2)$ values are indicated both for ^{132}Ba and for ^{134}Ba. The numbers in quotation marks are the relative values (branching ratios) for decays where the absolute values are not known. The parameters used for calculations are those from Table IV. The γ-ray experimental data are taken from Refs. [10,11].

were calculated. These calculations were performed with the computer code FTNT, which, for the $L = 0$ transfer operator, uses the leading order term proportional to the bosonic $\hat{s}$ operator [15]:

$$\hat{P}_\nu^{(0)} = \alpha_\nu \left(\Omega_\nu - N_\nu - \frac{N_\nu}{N} \hat{n}_d \right)^{\frac{1}{2}} \left(\frac{N_\nu + 1}{N + 1} \right)^{\frac{1}{2}} \hat{s}, \qquad (8)$$

where Ω_ν is the pair degeneracy of the neutron shell, N_ν is the number of neutron pairs, N is the total number of bosons, and α_ν is a constant parameter.

For ^{132}Ba, the calculation produced two excited 0^+ states in the excitation range below 3 MeV with significant (p,t) strengths. The first state, at 1372.3 keV, has 6.2% from that of the ground-state strength and the second, at 1753.3 keV, has 2.3% from the ground state. For ^{134}Ba, two excited 0^+

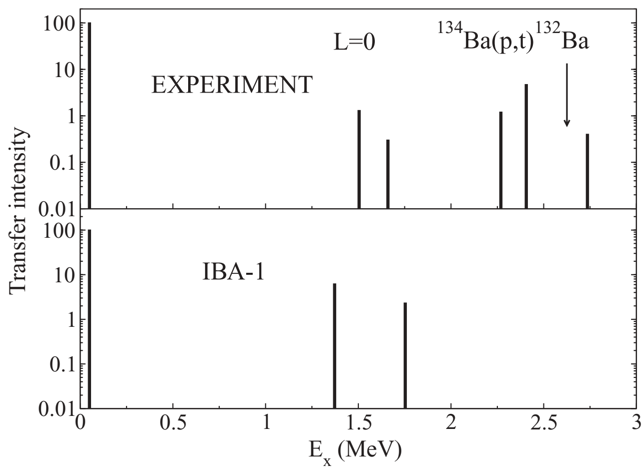

FIG. 6. Comparison of the measured $L = 0$ transfer intensities for the 0^+ states in ^{132}Ba with the IBA-1 predictions. Values are normalized to 100 corresponding to the $0_1^+(^{134}\mathrm{Ba}) \rightarrow 0_1^+(^{132}\mathrm{Ba})$ transition. The vertical arrow indicates the pairing gap calculated from the odd-even mass difference.

states with significant (p,t) strengths were also found in the same excitation range, at 1653.2 keV with an intensity of 0.7% from that of the ground-state strength and at 2041.9 keV with 1.6% from the ground state. Their comparison with the experimental results is shown in Fig. 6 for ^{132}Ba and in Fig. 7 for ^{134}Ba. The calculations provide a good description of the excitation energy and (p,t) strength for the first two excited 0^+ states.

The two-neutron transfer intensity to the 2^+ states was also calculated in this work. For the $0^+_{\mathrm{gs}} \rightarrow 2^+$ transitions, the $L = 2$ transfer operator used in FTNT contains three different terms, proportional to the $\hat{d}^\dagger$, $\hat{s}^\dagger(\hat{d}^\dagger\tilde{d})^2$, and $(\hat{s}^\dagger\hat{s}^\dagger\tilde{d})$ operators:

$$\hat{P}^{(2)}_{\nu,\mu} = \frac{N_\nu + 1}{N + 1}\left[\alpha\left(\Omega_\nu - N_\nu - \frac{N_\nu}{N}\hat{n}_d\right)^{\frac{1}{2}}\left(\frac{N_\nu + 1}{N + 1}\right)^{\frac{1}{2}}\hat{d}^\dagger_\mu + \beta\frac{(\Omega_\nu - N_\nu)^{1/2}}{\sqrt{5}}\hat{s}^\dagger(\hat{d}^\dagger\tilde{d})^{(2)} + \gamma(\hat{s}^\dagger\hat{s}^\dagger\tilde{d})\right], \quad (9)$$

where α, β, and γ are parameters.

The intensity of these transitions is computed as a coherent sum of the matrix elements of these three operators. In the

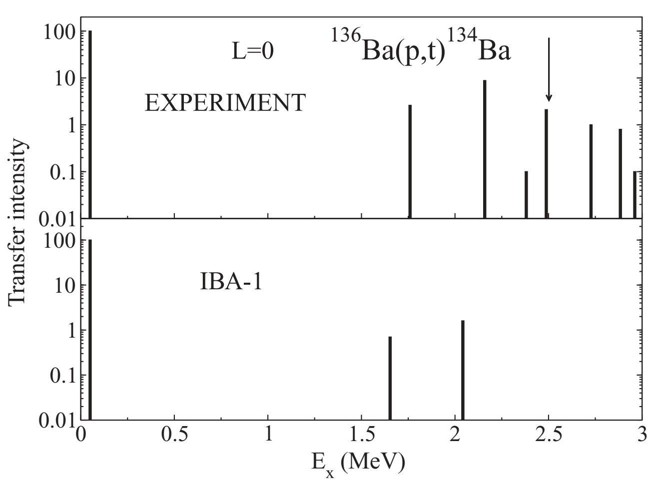

FIG. 7. Comparison of the measured $L = 0$ transfer intensities for the 0^+ states in ^{134}Ba with the IBA-1 predictions. Values are normalized to 100, corresponding to the $0_1^+(^{136}\mathrm{Ba}) \rightarrow 0_1^+(^{134}\mathrm{Ba})$ transition. The vertical arrow indicates the pairing gap calculated from the odd-even mass difference.

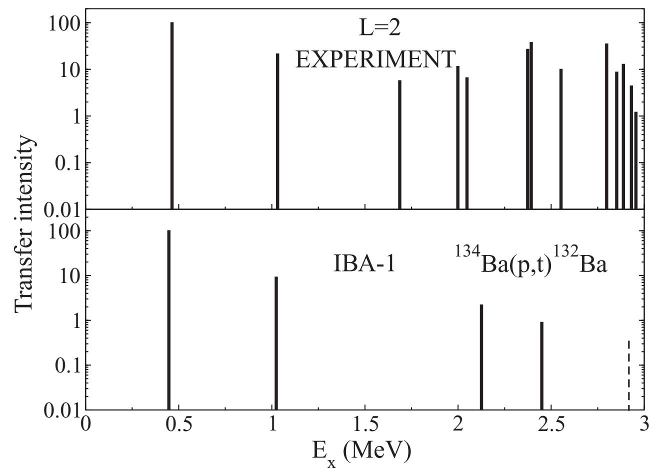

FIG. 8. Comparison of the experimental $2n$ transfer intensity for the 2^+ states and IBA-1 predictions. The intensities are normalized to the $0_1^+(^{134}\mathrm{Ba}) \rightarrow 2_1^+(^{132}\mathrm{Ba})$ transition. The vertical dashed line indicates the position of the next excited 2^+ state produced by the IBA-1 model. The FTNT code prohibits calculation of the $2n$ transfer matrix elements to more than four states.

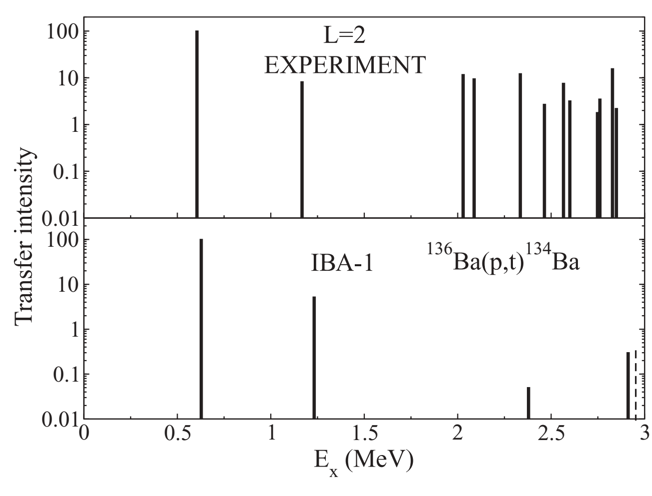

FIG. 9. Comparison of the experimental $2n$ transfer intensity for the 2^+ states and IBA-1 predictions. The intensities are normalized to the $0_1^+(^{136}\mathrm{Ba}) \rightarrow 2_1^+(^{134}\mathrm{Ba})$ transition. The vertical dashed line indicates the position of the next excited 2^+ state produced by the IBA-1 model. The FTNT code prohibits calculation of the $2n$ transfer matrix elements to more than four states.

lower panel of Figs. 8 and 9, the model estimations are presented for $L = 2$ two-neutron transfer intensity for ^{132}Ba and ^{134}Ba, respectively, by considering equal values for the parameters α, β, and γ. In ^{132}Ba, up to 2 MeV, four 2^+ states are observed in the present experiment with excitation energies of 464.5, 1031.5, 1687.1, and 1998.7 keV, respectively. Their transfer strengths, normalized to that of the first excited 2^+ state, are 100%, 21.4%, 5.7%, and 11.5%, respectively. As can be observed from Fig. 8, the first three states show that the calculated (p,t) transfer intensities are in rather good agreement with experiments; that is, the model places the first three 2^+ states at energies of 447.0, 1023.7, and 2125.8 keV, with the calculated intensities of 100%, 9.2%, and 2.2%, respectively. In ^{134}Ba, up to 2.1 MeV, four 2^+ states are observed in the present experiment with excitation energies of 604.8, 1167.7, 2029.2, and 2087.8 keV, respectively. Their transfer strengths, normalized to that of the first excited 2^+ state, are 100%, 8.2%, 11.7%, and 9.5%, respectively. As can be observed from Fig. 9 for the first two states, the calculated (p,t) transfer intensities are also in good agreement with experiment; that is, the model places the first two 2^+ states at energies of 627.9 and 1232.1 keV, with the calculated intensities of 100% and 5.2%, respectively. Also the simple picture of the O(6) limit predicts the second excited 2^+ state with a (p,t) intensity of ~20% from the first excited 2^+ state and a vanishing one for the third excited 2^+, which is in good agreement with our experimental data. Up to 3 MeV, the model predicts three other 2^+ states that do not have a clear correspondence with any experimental state.

Both $L = 0$ and $L = 2$ two-neutron transfer intensity patterns for the low-lying states are consistent with the IBA-1 model predictions for a transitional region between the U(5) and O(6) dynamic symmetries. The role of the mixing of the collective states with the intruder (quasiparticle) states may be of major importance in understanding the structure of ^{132}Ba and ^{134}Ba near the pairing gap, as discussed for other even-even Ba isotopes (Ref. [7] and therein).

V. CONCLUSIONS

In summary, ^{132}Ba and ^{134}Ba nuclei were experimentally investigated using the (p,t) reaction at an incident energy of 25 MeV. The tritons were analyzed with the Q3D spectrograph and recorded with a high-resolution focal-plane detector. The analysis of the triton spectra allowed the observation of 47 new levels below 4.2 MeV for ^{132}Ba and 34 new levels below 3.9 MeV for ^{134}Ba. For some of these states, a spin assignment was made. Both the energy and the spin for most of the previously known states were confirmed. The experimental two-neutron transfer strengths of the low-lying 0^+ and 2^+ states were compared with predictions of the IBA-1 model. Calculations were carried out by using a new set of model parameters determined to describe electromagnetic and (p,t) data simultaneously. These calculations confirm previous conclusions of γ-ray spectroscopy studies that the structure of the ^{132}Ba and ^{134}Ba nuclei is between U(5) and O(6) dynamic symmetries.

ACKNOWLEDGMENTS

We thank the Tandem accelerator staff of the Maier-Leibnitz Laboratory for the excellent conditions during the experiment. We acknowledge partial support from the Deutsche Forschungsgemeinschaft under Grant No. II C4-Gr 894/2, from Consililul National al Cercetarii Stiintifice din Invatamantul Superior (CNCSIS) under Contract Nos. ID-117/2007, ID-118/2007, and ID-180/2007, and from Centrul National de Management Programe (CNMP) under Contracts Nos. PNCDI II 71-042/2007 and 71-051/2007.

[1] R. F. Casten and P. von Brentano, Phys. Lett. **B152**, 22 (1985).
[2] F. Iachello and A. Arima, *The Interacting Boson Model* (Cambridge University, Cambridge, England, 1987).
[3] R. F. Casten and N. V. Zamfir, Phys. Rev. Lett. **85**, 3584 (2000).
[4] S. Pascu, Gh. Căta-Danil, D. Bucurescu, N. Mărginean, N. V. Zamfir, G. Graw, A. Gollwitzer, D. Hofer, and B. D. Valnion, Phys. Rev. C **79**, 064323 (2009).
[5] Gh. Căta-Danil, D. Bucurescu, L. Trache, A. M. Oros, M. Jaskola, A. Gollwitzer, D. Hofer, S. Deylitz, B. D. Valnion, and G. Graw, Phys. Rev. C **54**, 2059 (1996).
[6] R. F. Casten and D. D. Warner, Rev. Mod. Phys. **60**, 389 (1988).
[7] G. Suliman, D. Bucurescu, R. Hertenberger, H. F. Wirth, T. Faestermann, R. Krücken, T. Behrens, V. Bildstein, K. Eppinger, C. Hinke, M. Mahgoub, P. Meierbeck, M. Reithner, S. Schwertel, and N. Chauvin, Eur. Phys. J. A **36**, 243 (2008).
[8] H. J. Scheerer, H. Vonach, M. Löffler, A. v. d. Decken, M. Goldschmidt, C. A. Wiedner, and H. A. Enge, Nucl. Instrum. Methods **136**, 213 (1976).
[9] R. Hertenberger, H. Kader, F. Merz, F. J. Eckle, G. Eckle, P. Schiemenz, H. Wessner, and G. Graw, Nucl. Instrum. Methods Phys. Res. A **258**, 201 (1987).
[10] Yu. Khazov, Nucl. Data Sheets **104**, 497 (2005).
[11] A. A. Sonzogni, Nucl. Data Sheets **103**, 1 (2004).
[12] N. K. Glendenning, *Direct Nuclear Reactions* (Academic Press, New York, 1983).
[13] P. D. Kunz, Zero Range Distorted Wave Born Approximation, University of Colorado (unpublished).
[14] F. D. Becchetti Jr. and G. W. Greenlees, Phys. Rev. **182**, 1190 (1969).
[15] O. Scholten, program packages PHINT, FBEM, and FTNT (unpublished).
[16] G. Puddu, O. Scholten, and T. Otsuka, Nucl. Phys. **A348**, 109 (1980).
[17] P. Petkov, A. Dewald, and W. Andrejtscheff, Phys. Rev. C **51**, 2511 (1995).
[18] W. T. Chou, N. V. Zamfir, and R. F. Casten, Phys. Rev. C **56**, 829 (1997).
[19] A. A. Sonzogni, Nucl. Data Sheets **95**, 837 (2002).